

Received December 30, 2020, accepted January 11, 2021, date of publication January 22, 2021, date of current version February 5, 2021.

Digital Object Identifier 10.1109/ACCESS.2021.3053858

# A Non-Intrusive Deep Learning Based Diagnosis System for Elevators

**SONGJIAN CHAI<sup>ID1</sup>, (Member, IEEE), XURAN IVAN LI<sup>2</sup>, YOUNWEI JIA<sup>ID3,4</sup>, (Member, IEEE), YUFEI HE<sup>ID5</sup>, (Member, IEEE), CHI HO YIP<sup>2</sup>, KA KEI CHEUNG<sup>2</sup>, AND MINGHAO WANG<sup>5</sup>, (Member, IEEE)**

<sup>1</sup>College of Physics and Optoelectronic Engineering, Shenzhen University, Shenzhen 518060, China

<sup>2</sup>Electrical and Mechanical Services Department, Government of the HKSAR of the PRC, Hong Kong

<sup>3</sup>Ergatian Limited, Hong Kong

<sup>4</sup>Department of Electrical and Electronic Engineering, Southern University of Science and Technology, Shenzhen 518055, China

<sup>5</sup>Department of Electrical Engineering, The Hong Kong Polytechnic University, Hong Kong

Corresponding author: Minghao Wang (minghao.wang@polyu.edu.hk)

This work was supported by Electrical and Mechanical Services Department, the Government of the HKSAR of the PRC under Grant 4200397034.

**ABSTRACT** With the ever-growing number of elevators coupled with the aging workforce, diminishing new installations and limited use of maintenance technology, it is increasingly challenging for the owners and responsible parties to maintain the safe and reliable operation of the lift systems. To address this issue, a non-intrusive artificial intelligence (AI) based diagnosis system, aiming at providing fault detection and potential fault prediction for multi-brand lifts without intervening the existing circuitry of the lift installations, is proposed in this paper. The proposed system employs the multivariate long short term memory fully convolutional network (MLSTM-FCN) to learn and analyze the measured signals from the non-intrusive detection system of the elevators. It is capable of (i) giving advance and clear warnings of corrective actions to prevent major equipment breakdowns, and (ii) indicating just-in-time maintenance for enhancing the lift reliability at a low cost. The implementation of the non-intrusive detection system is provided. The design of the diagnostic algorithm is elaborated. Both the simulations and experiments of a commercial elevator have been conducted to verify the effectiveness of the proposed system.

**INDEX TERMS** Deep learning, electric traction system, fault detection, elevator system, artificial intelligence.

## I. INTRODUCTION

### A. BACKGROUND

Elevators have been massively installed in the mansions, factories, cargo piers and etc. As an important tool for transporting passengers and delivering cargos, its reliability is vital to the safety of human beings and economic development. To increase the robustness of the lift system, the design of reliable traction motor, robust motor control schemes and protection systems have been developed. However, considering the complexity of the elevator system, which consists of the traction motor, lift car, brake and door motor, the reported research on the reliability improvement of the lift systems is insufficient. Besides, the practical maintenance of elevator is either performed periodically or conducted after failure of the lifts, which may involve excessive maintenance costs and unnecessary service interruptions. To resolve this issue,

the intrusive transducers such as weighbridge, speed encoder and etc., have been installed in the elevators to detect the operating condition of the lift car. Although these method are of relatively low cost and can provide measurements for professionals to analyze the potential failure, the installation and maintenance of intrusive transducers demand will interrupt the services of the lift and extra overheads must be paid to professionals for conducting repetitive data analysis. Furthermore, transfer or communication may be hindered due to proprietary software or different communication protocols developed by lift manufacturers. To tackle the reliability issue fundamentally, a general non-intrusive monitoring and diagnosis system for the elevator system is required [1].

Considering it is the installation of sensors or replacements, maintenance and repair that interrupt the service of the lift, the monitoring of lift is preferred to impose the minimum impacts on the lift, i.e., the entire process must be nonintrusive. Besides, the diagnosis should be totally automatic and involves little human participation for avoiding the human

The associate editor coordinating the review of this manuscript and approving it for publication was Jiayong Li.

error and reducing overheads. The main difficulties for this diagnosis of the lift condition lie in three aspects, namely, (i) the measurements of key parameters without interruption and intrusion of the lift installation, (ii) lack of professional knowledge for identifying the potential failure with limited information, and (iii) lack of monitoring database for consistent supervision of lift condition. Since the monitor panels, interfacing software and deployed sensors of lifts are different across all kinds of brands and generations, it is difficult established a generalized platform for condition diagnosis by utilizing the existing infrastructure. Particularly, considering the early-installed lift systems with limited embedded or worn-out sensors, considerable work load must be paid on the deployment of intrusive sensors in the lift well and ect. This leads to not only the extra cost but also the suspension of lift service. Alternatively, non-intrusive sensors can be deployed in the machine room for obtaining the limited and indirect measurements of the lift. However, with the obtained limited information, the professional knowledge of the lift system, typically an accurate physical model of the lift system, is required for performing accurate diagnosis. This is time consuming and difficult. Besides, the long-term operation of the lift can lead to the change of its physical condition, which requires a database to track this change. In recognition of these challenges, considering the outstanding performances of the AI technologies in pattern identification and model recognition, it is worth implementing with the non-intrusive sensors to achieve the monitoring and diagnosis of lift conditions.

## B. LITERATURE REVIEW

In recent years, a plethora of efforts have been devoted to the condition monitoring and fault diagnosis in various industrial processes and machinery [2], [3]. However, the elevator well-being monitoring or fault detection has been scarcely touched. Generally, the existing condition monitoring techniques for elevator or elevator components can be broadly classified into two categories, namely model-based and data-driven approaches. E. Esteban *et al.* [4] proposed a model-based strategy to estimate the mechanical energy losses due to the rail friction forces during the ride, as well as whole installation efficiency, where a Linear Parameter Varying (LPV) model of a 1:1 elevator installation was employed. In a subsequent work [5], the authors presented a state space model to represent the dynamics of elevator system, including both electrical and mechanical processes. This model was reported to be valid for estimating the ride quality key performance indicators. A remote monitoring setup was developed in [6] to measure the machine room temperature and vibration parameters, where the abnormal conditions were informed by simply setting a severity limit according to experience. In such model-based schemes, a prior physical and mathematical knowledge of the elevator operational process is always required. Nevertheless, due to a large variety of elevators of different brands flood into the market nowadays,

acquiring explicit parameters and models of specific elevators becomes rather difficult. On the other hand, the data-driven approaches have drawn increasing attention recently as it doesn't require any prior knowledge of elevator systems. Literature [7] presented a performance evaluation model for elevator door motion system. The data was acquired via an encoder to measure door displacement and parallel connections. The logistic regression model was used to establish the mapping between inputs (open cycle times and maximum angular speed) and output (probability of failure). In [8], three variants of support vector machine (SVM) model were applied for diagnosing vibration signals of an elevator door. The experiment was carried out by considering 10 faulty conditions. A (magnetic flux leakage) MFL-based method for flaw defects in steel wire rope was presented in [9], which is based on a differential signal from a pair of sensors for each encapsulated rope. Z. Wan *et al.* [10] collected the vibration signals of elevator and used least square SVM (LS-SVM) to identify the causes of malfunctions, including deviated elevator guide rail, deviated shape of guide shoe, abnormal running of tractor, erroneous rope groove of traction sheave, deviated guide wheel, and tension of wire rope. This approach relies on wavelet transform to extract the necessary feature vectors of signals. A traction motor dedicated fault detection method based on decision fusion system was introduced in [11]. The vibration signal and current signal were both measured to give a comprehensive inspection. Various features regarding the time domain and frequency domain were extracted to establish the fault classifier on the basis of a collection of models, including SVM, k-nearest neighbors (k-NN), random forest. Finally, 9 typical faulty types of motor can be identified with high accuracy. A most recent work [12] proposed an IoT elevator monitoring system via smart sensor modes (accelerometer and magnetometer). Through using different signal processing schemes without training, various abnormalities (e.g., emergency stops, abnormal door behavior) can also be effectively identified.

However, it is found that most of the existing elevator condition monitoring approaches were developed based on the vibration parameters measured from e.g., accelerometers, while the electric signals taken from main electric components were seldom investigated. This idea was inspired by the smart meter that can tell the energy utilization pattern and efficiency of the energy use. Likewise, the current flowing at main elevator circuits (e.g., traction motor, brake, door and safety circuit) is informative as well to tell the healthiness of elevator. In addition, most of the state-of-the-arts data-driven models tend to apply shadow machine learning models (e.g., SVM) with extra feature engineering efforts to construct the fault diagnosis model. During the past few years, deep learning models have been pervasively used in a variety of data-driven problems as it is capable of extracting features by itself during learning process. The ‘invisible’ or complicated features involved in the dataset can always be effectively uncovered by such models.

### C. CONTRIBUTION OF THIS WORK

In light of above, this paper presented a deep learning based lift well-being monitoring and diagnosis framework using current signals of main electric components. The proposed framework aims at providing fault detection and potential fault prediction for multi-brand lifts without intervening the existing circuitry of the lift installations. This framework consists of three parts (i) non-intrusive sensing system, (ii) data collection and management system and (iii) An AI diagnosis system. Different types of sensors are introduced to detect the responses of the lift system when it is affected by these potential failures. The hardware setup of the monitoring system is elaborated. The design of the AI diagnosis system is discussed. We adopted a well-established deep learning model - **MLSTM-FCN** [13] to learn and predict the likely faults or abnormalities. This model leverages the advantages of both sequence network and convolutional network, which has achieved great success in various tasks for multivariate sequence classification, such as activity recognition or fraud detection. The functionalities of this non-intrusive monitoring system are verified through simulations and actual hardware experiments.

The merits of the proposed non-intrusive condition monitoring and fault diagnosis system lie in three-fold, (i) The monitoring framework can be implemented without intervening any component of original system, which could be also expanded flexibly with more sensors; (ii) It is completely model-free, neither physical nor mathematical model representations are required under the proposed framework; (iii) It is computational efficient. Distinguishing from traditional feature-based algorithms, the **MLSTM-FCN** doesn't require sophisticated and expensive feature extraction processes, such as Fast Fourier Transform (FFT). The collected signals can be directly fed into the model with little preprocessing.

The remainder of this paper is organized as follows. The holistic non-intrusive lift monitoring framework is presented in Section II. Signal preprocessing and abnormal sequence generation is described in Section III. Section IV covers the theoretic background of **MLSTM-FCN**. The experiment is detailed in Section V. The last section includes some conclusion remarks and outlines the possible extensions.

## II. NON-INTRUSIVE LIFT MONITORING FRAMEWORK

### A. HOLISTIC MONITORING FRAMEWORK

The structure of the proposed non-intrusive AI-based diagnosis system can be plotted as shown in Fig. 1. It can be used for monitoring the lift operating conditions and providing fault prediction for multi-brand lifts without intervening the existing hardware and software of the lift installations, therefore enabling the cross-platform applicability. This system comprises (i) non-intrusive voltage/current sensors configured to acquire real-time electric voltage/current signals of the traction motor, brake coil, door motor and safety circuit of lifts, (ii) a microcontroller (e.g. Raspberry PI and Adruino)

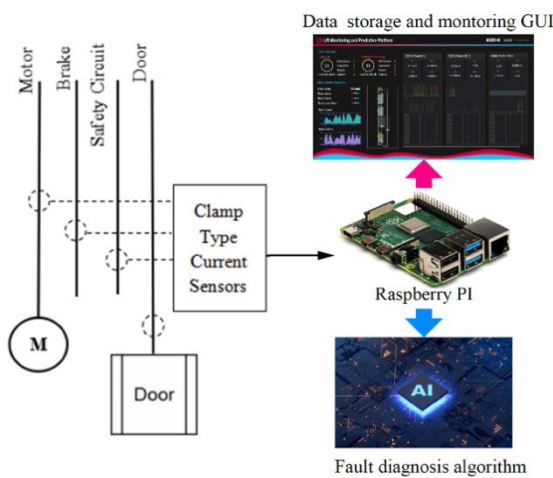


**FIGURE 1.** The structure of the proposed non-intrusive AI-based diagnosis system.

**TABLE 1.** Pros and Cons of PMS and Asynchronous Motors

Faulted Parts	PMS Motor	Asynchronous Motor
Rotor Speed	Constant	Affected by load
Cost	High	Low
Overloading Capability	Low	High
Volume	Small	Large
Reliability	Low	High

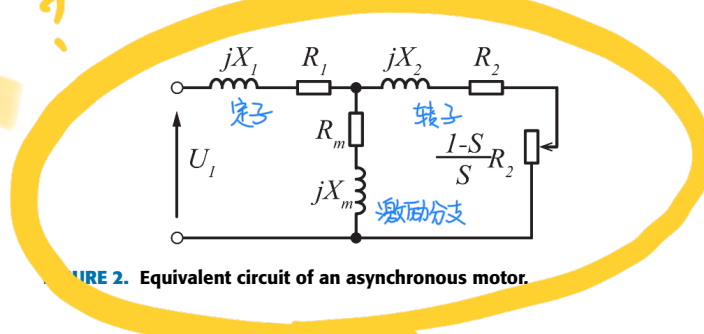


**FIGURE 2.** Equivalent circuit of an asynchronous motor.

configured to fetch the electric signals from the non-intrusive sensors and then transfer the data to servers, and (iii) a server configured to store the collected signal data, and analyze the data based on artificial intelligence to diagnose the operating conditions of lifts.

### B. MEASURED COMPONENTS

#### 1) MOTOR

Both the permanent magnet synchronous (PMS) motor and the AC asynchronous motor can be applied as the traction motor of the elevators. The pros and cons of these two types of motors are summarized as shown in Table 1.

Due to the relative low cost and high reliability of the asynchronous motors, they are widely applied in the lift systems.

The equivalent circuit of the asynchronous motors can be plotted as shown in Fig. 2, where  $S$  is the slip ratio.  $R_1 + jX_1$ ,  $R_2 + jX_2$  and  $R_m + jX_m$  are the equivalent impedances of the stator, rotor and excitation branch, respectively. Based on

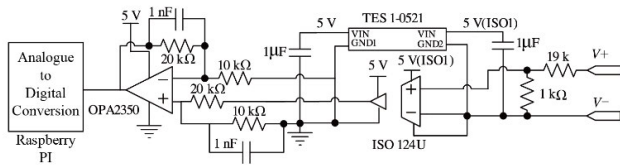


**FIGURE 3.** Electronic circuit schematic diagram of a non-intrusive isolated voltage sensor.

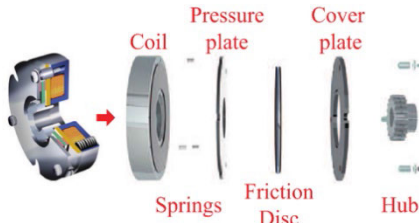


**FIGURE 4.** Structure of a magnet power-off brake.

the equivalent circuit shown in Fig. 2, the output mechanical power is essentially the power dissipated on the equivalent resistor of  $R_2/S$ . If the voltage quality of  $U_1$  is poor, it can be conceived that the power of  $R_2/S$  will be fluctuating, which affects the mechanical torque of the motor. As a consequence, the input voltage of  $U_1$  is a critical indicator for the operation of the motor. To achieve a non-intrusive detection and monitoring of  $U_1$ , an isolated differential voltage transducer can be applied. The typical design of this sensor can be plotted as shown in Fig. 3.

As illustrated in Fig. 3, the measured voltage will be stepped down by a resistive voltage divider proportionally. Then, the isolated linear amplifier of ISO 124U is used to transform the scaled-down voltage in a linear and isolated way. At last, the operational amplifier is applied to tune the measured voltage to an acceptable voltage level for the analogue to digital conversion (ADC) of the Raspberry PI. By using this non-intrusive isolated voltage sensor, the potential voltage fluctuation of  $U_1$  will not damage the Raspberry PI. Meanwhile, the possible faults of the sensing circuit will not affect the voltage quality of  $U_1$ .

## 2) BRAKE

The magnetic power-off brakes are generally applied in the elevator systems. The typical structure of this brake can be plotted as shown in Fig. 4. When the elevator is halted, the power supply of the coil is cut-off and the coil is demagnetized. The tensioned springs will push the pressure plate to lock the friction disk in between the pressure plate and the cover plate. The friction disk, the hub and the shaft are tightly connected. The induced friction of the friction plate will finally stop the motion of the shaft and the lift. When the elevator is started, the coil will be powered up to magnetize the coil. The electromagnetic force will pull the pressure plate towards the coil and release the friction disc. Then, the shaft can rotate to move the lift car. Practically, the possible faults can be summarized as shown in Table 2.

**TABLE 2. Summary of Brake Faults**

Faulted Parts	Effect	Motion of Lift
Springs	Insufficient friction	Slowed deceleration
Coils	Reduced magnetism	Slowed acceleration
Friction disk	Insufficient friction	Slowed deceleration

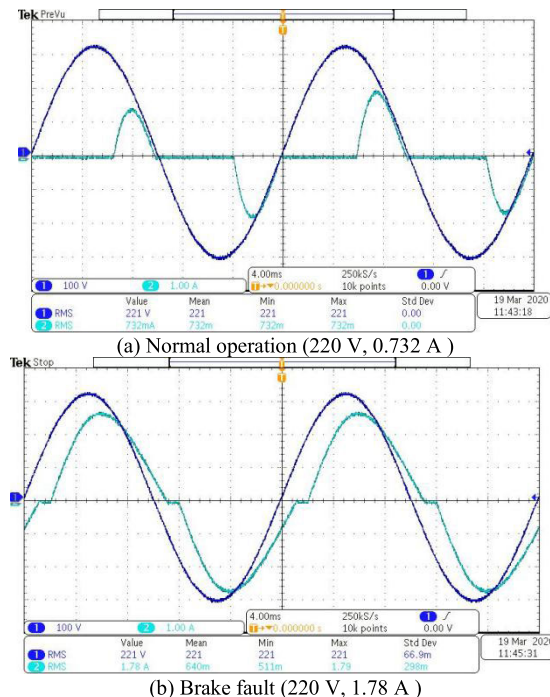


**FIGURE 5.** Experimental waveforms of brake motor in (a) normal condition and (b) brake fault condition.

As illustrated in Table 2, the faults of springs, coil and friction disk will eventually affect the motion of the lift car, which degrades its performance and threat the safety. Considering the diversity of lift weights, lift brands, motors and etc., it is very difficult to use a predefined model to differentiate the abnormal operating conditions from the normal ones, not even mentioning to identify the actual faulted components of the brake.

Considering the possible fault cases shown in Table 2, the malfunctions of brake will eventually affect the current of the motor. As an illustration, the experimental waveforms of the motor in normal and brake fault conditions can be shown in Fig. 5.

Comparing Fig. 5(a) and 5(b), when the brake coil is faulted, the motor current will be increased significantly. This is due to the faulted brake jamming the rotor. As a result, the stator current will surge.

Besides, the current of the brake can also reflect the operating status of the brake. Instead of monitoring the status of the mechanical parts of the brake, two non-intrusive current sensors are deployed to monitor the current amplitudes of the

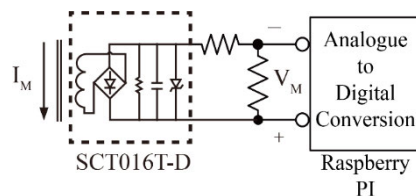


**FIGURE 6.** Electronic circuit schematic diagram of a non-intrusive isolated current sensor.

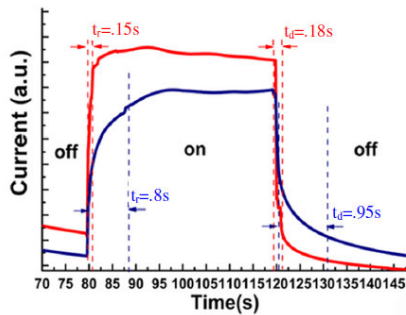


**FIGURE 7.** Typical current response of the safety link due to open and closing of safety contacts.

motor and the brake coil. A typical isolated current sensing circuit can be applied as shown in Fig. 6.

As shown in Fig. 6, a voltage type current transformer SCT016T-D is applied to transform the AC current signal to the DC voltage. The amplitude of the targeted current  $I_M$  will be proportional to the output DC voltage  $V_M$ . This DC voltage  $V_M$  will be finally detected by the Raspberry PI before being scaled down by a voltage divider. Similarly, with the use of current transformer, the main circuit is electrically isolated from the sensing circuit and the mutual interference between the main circuit and sensing circuit can be prevented.

### 3) SAFETY CIRCUIT

To ensure the safe operation of the lift system, protective safety link or safety circuit, which is essentially a series connected chain of safety relay, electric power supply and etc., is applied to avoid the malfunction of the lift. The disconnection of safety link will lead to the notch-off of the lift system immediately. Fig. 7 shows the typical current waveforms of the safety link during relay opening operation and closing operation. As a vital indicator of the lift operating condition, the current signal of the safety circuit can potentially reflect the operating condition of the lift. Based on this consideration, a non-intrusive current sensor (see Fig. 6) is deployed to obtain the current signal of the safety circuit.

### 4) DOOR

The door of the lift is driven by a door motor. Both the PMS motor and the asynchronous motor can be applied as a door motor. By detecting the stator current of the door motor, the opening times, friction of lift door and etc, can

be observed. Similarly, this stator current can be measured by using the aforementioned current sensor as shown in Fig. 6.

## C. DATA ACQUISITION SYSTEM BASED ON RASPBERRY PI

The microcontroller is developed in the data acquisition system to fetch the electric current signals from the non-intrusive current sensors, converts the signals into predetermined formats and transfer to the servers. The data acquisition system can be developed based on but not limit to Raspberry PI, which is a single-board LINUX operation basde computer. The processor speed of the raspberry PIs ranges from 700 MHz to 1.4 GHz, which is sufficient for the signal processing. Besides, it provides different communication portals and general purpose input/output (GPIO) terminals, which is capable of incorporating different types of sensors via different communication portals. However, it has limited memory, which is not suitable of integrating the AI diagnosis algorithm. In the proposed system, the Raspberry PI is deployed as a data management system to interlink the server and the non-intrusive sensing system. In other words, all deployed sensors will deliver the analogue measurements to the ADC terminals of the Raspberry PI. Imbedded with the filtering algorithms, the Raspberry PI will perform the preconditioning of the raw data and send them to the server via WIFI network. In the server, the upper level visualization and analysis algorithm will be programmed and implemented to provide a systematic illustration of the lift condition.

## III. DATA PREPROCESSING

### A. DATA DESCRIPTION

The dataset we used was collected from a VVVF lift manufactured by Fujitech, which is installed in EMSD Headquarter, Hong Kong. Specifically, four current signals were recorded covering the period from 1 Mar 2019 to 31 May 2020 with the sampling frequency of 20 Hz, including the traction motor current, brake current, safety circuit current and door motor current. All data are normalized to have zero mean and unit variance before training.

### B. SIGNAL PARTITION

The collected current signals were then partitioned into a set of homogeneous operational segments to build multivariate samples for the subsequent model learning. Fig. 8 illustrates the partitioned results for a slice of measured current signals. Each operational segment starts at the moment when brake releases and ends when brake reopens. Hence, each cycle comprises two motions, i.e., elevator car motion and door motion. After removing the segments in maintenance days as well as those with loss measurements, totally 38367 measured multivariate sequences were obtained eventually.

### C. GENERATION OF ABNORMAL SEQUENCES

In order to perform the early fault prediction, collecting the anomaly measurements is crucial under the supervised

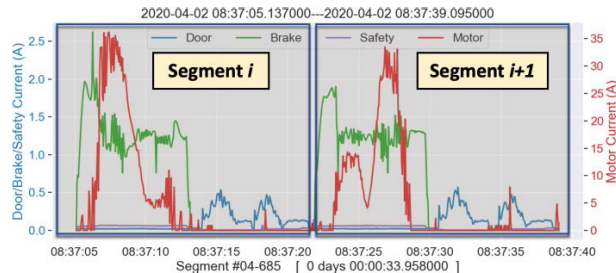


**FIGURE 8.** Sample construction by extracting elevator operational cycles.

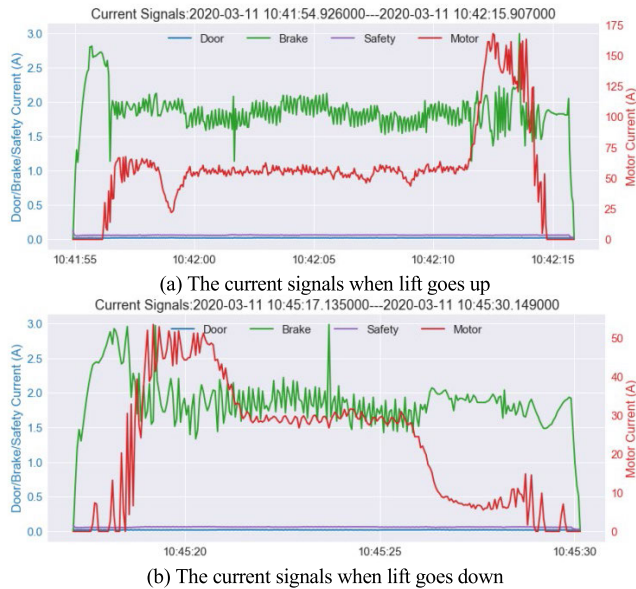
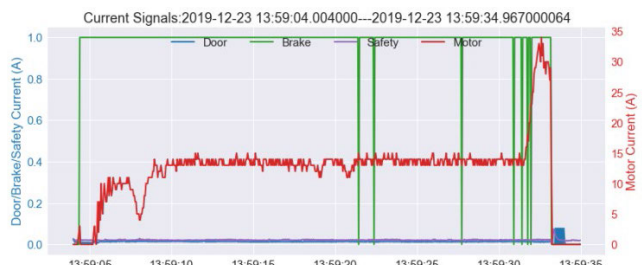


**FIGURE 9.** The lift current signals when brake is not fully opened.

learning framework. However, the elevator malfunction cases are seldom to happen in practice, while most of the lift conditions are healthy. In this regard, it is desirable to include some synthetic anomaly scenarios for sample enrichment. In this experiment, in order to facilitate the training process of the deep learning model, we manually created some abnormal current signals based on three typical irregular conditions, namely brake is not fully opened, grid voltage dip and abnormal door closing. The first one was obtained by field experiments, that is we slightly alter the brake spring to impede the brake from fully opening. While the other two scenarios were observed in real-life cases. The detail of each anomaly is illustrated as follows.

### 1) BRAKE IS NOT FULLY OPENED

This case was simulated by setting the brake spring to be more compressed so that when current pass through the brake coil, it does not have enough power to counteract the spring to make the brake fully open. This manipulation will lead to the increase of both brake and traction motor current when lift travels. As noted in Fig. 9, the brake current has been augmented to about 2.5A, which is more than 1.5 times the raw brake current. On the other hand, the traction motor needs



(a) The current signals measured on the target elevator at around 2:00pm on 23 Dec 2019

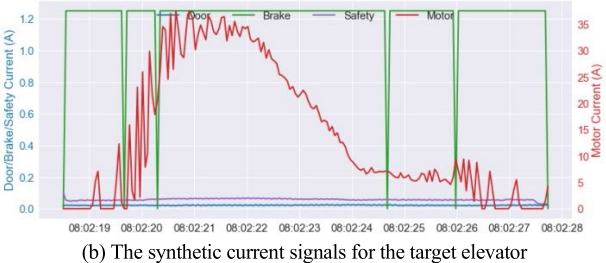


**FIGURE 10.** The lift current signals when grid voltage dips.

more energy to counteract this resistance, rendering a nearly five-fold increase of motor current when lift goes up (see Fig. 9 (a)), and about 1.5 times the raw motor current when lift goes down (see Fig. 9 (b)). Following such rules, we create 60 alike samples when the brake is not fully opened.

### 2) GRID VOLTAGE DIP

On 23 Dec 2019, dozens of passengers trapping accidents and elevator breakdown events have been reported in Hong Kong due to a transient voltage dip of main grid occurred in east Kowloon at around 2:00pm. The resultant current profile of the target elevator within this period is recorded in Fig. 10 (a). As one may notice that the brake current flattens out at a constant level with several negative ramps. To enrich the samples with respect to this situation, we randomly picked 20 segments and amend the brake current therein by flattening it out at its average along with several zero noises, Fig. 10 (b) depicts one of the generated sequences when grid voltage dips.

### 3) DOOR CLOSING ISSUE

In normal situations, the door motor should be energized to open and close the elevator door shortly after the elevator car stops. This process can be visually displayed by two consecutive current waveforms, see Fig. 8 (the blue lines). Each waveform represents one motion of the elevator door. However, irregular motions may occur in some elevators that when you press the closing door button, it fails to fully close the door. Instead, the opened elevator door only pops up for a small portion (see Fig. 11 (a)) and rapidly back to its fully opened status. This phenomenon has been recorded in another Fujitech elevator in the same building. One of the resultant current profile is illustrated in Fig. 11 (b), as clearly can be seen, there are three consecutive waveforms in this situation, where the middle one is likely to trigger the door motor to

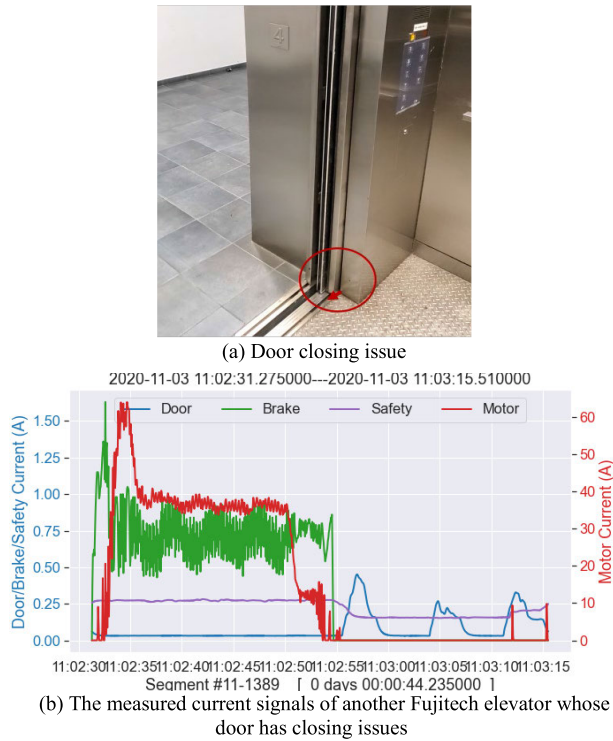


**FIGURE 11.** Door closing problem happened in another Fujitech elevator.

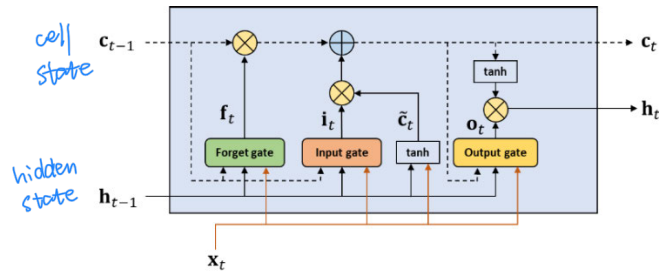


**FIGURE 12.** Inner configuration of LSTM unit

close the door but fails, while the last waveform indicates the door is fully closed afterwards. Totally 120 analogous samples with respect to this anomaly are collected for the subsequent model learning and validation.

#### IV. MULTIVARIATE LSTM-FCN

##### A. LSTM WITH ATTENTION MECHANISM

Multivariate LSTM-FCN leverages the merits of LSTM network to exploit the temporal dynamics involved in the current signals. As a variant of recurrent neural network (RNN), LSTM allows to share the features learned across the timeline and successfully addresses the issue of vanishing gradients by integrating gating functions into their state dynamics [14]. A typical schematic of the standard LSTM unit is portrayed in Fig. 6.

The distinguishing feature of LSTM is the introduction of cell state  $\mathbf{c}_t$  (the dashed line in Fig. 12), which overcomes the gradient vanishing issue in RNN and allows to memorize certain information over history. The memory cell acts

as an accumulator of the state information, in the process of network forward propagation, the cell state is accessed, written and cleared by three sigmoid function governed gates, namely forget gate, input gate and output gate. At each time step, there are three vectors fed into the current unit, i.e., the previous cell state  $\mathbf{c}_{t-1}$ , the previous hidden state  $\mathbf{h}_{t-1}$  and the present input  $\mathbf{x}_t$ . These inputs pass through each gate to output the vectors  $\mathbf{f}_t$ ,  $\mathbf{i}_t$  and  $\mathbf{o}_t$  that are between 0 and 1 for each vector element. The forget gate decides what information needs to remove from the old cell state by  $\mathbf{f}_t \circ \mathbf{c}_{t-1}$ , where ‘ $\circ$ ’ denotes the Hadamard product. The input gate decides which values that are going to update, here a vector of new candidate state  $\tilde{\mathbf{c}}_t$  is generated by a ‘tanh’ layer, then an element-wise multiplication  $\mathbf{i}_t \circ \tilde{\mathbf{c}}_t$  is implemented to decide what new information is going to store in the cell state. The cell state is subsequently updated by combining them together, i.e.,  $\mathbf{c}_t = \mathbf{f}_t \circ \mathbf{c}_{t-1} + \mathbf{i}_t \circ \tilde{\mathbf{c}}_t$ . The output gate decides what parts of the cell state are expected to output, by further multiplying by the updated cell state through ‘tanh’, i.e.,  $\mathbf{h}_t = \mathbf{o}_t \text{tanh}(\mathbf{c}_t)$ , a filtered cell state vector is derived as the output. Usually, more LSTM units are stacked and temporally concatenated to form a deeper and more complicated network to better exploit the complex relationships between inputs and outputs. The equations governing a single LSTM unit can be written as,

$$\begin{aligned} \mathbf{i}_t &= \sigma(W_{xi} \cdot \mathbf{x}_t + W_{hi} \cdot \mathbf{h}_{t-1} + W_{ci} \circ \mathbf{c}_{t-1} + b_i) \\ \mathbf{f}_t &= \sigma(W_{xf} \cdot \mathbf{x}_t + W_{hf} \cdot \mathbf{h}_{t-1} + W_{cf} \circ \mathbf{c}_{t-1} + b_f) \\ \tilde{\mathbf{c}}_t &= \tanh(W_{xc} \cdot \mathbf{x}_t + W_{hc} \cdot \mathbf{h}_{t-1} + b_c) \\ \mathbf{c}_t &= \mathbf{f}_t \circ \mathbf{c}_{t-1} + \mathbf{i}_t \circ \tilde{\mathbf{c}}_t \\ \mathbf{o}_t &= \sigma(W_{xo} \cdot \mathbf{x}_t + W_{ho} \cdot \mathbf{h}_{t-1} + W_{co} \circ \mathbf{c}_{t-1} + b_o) \\ \mathbf{h}_t &= \mathbf{o}_t \circ \tanh(\mathbf{c}_t) \end{aligned} \quad (1)$$

where  $[W_{xi}, W_{hi}, W_{ci}], [W_{xf}, W_{hf}, W_{cf}], [W_{xc}, W_{hc}]$  and  $[W_{xo}, W_{ho}, W_{co}]$  are weight matrices of input gate, forget gate, new cell and output gate, respectively.  $b_i, b_f, b_c$  and  $b_o$  refer to biases of input gate, forget gate, new cell and output gate, respectively.  $\sigma$  denotes the sigmoid activation function.

The standard LSTM network is difficult to capture very long-term dependency due to its memory update mechanism which keeps erasing previous memories and refreshes with new observations [15]. This imposes great challenges to our problem, since the current signals are always characterized by long length. To resolve this problem, we augment the standard LSTM with attention mechanism. This idea was originally proposed by Bahdanau *et al.* [16] to address the forgetful issues in long text translation. The attention model can not only embed all the input words while creating the context vector, but take into account the relative importance by assigning different weights to each one of them. Put another way, all hidden states in encoder are examined to give the predicts instead of only considering the last one in the conventional sequence model. Suppose the context vector for  $i$ -th output

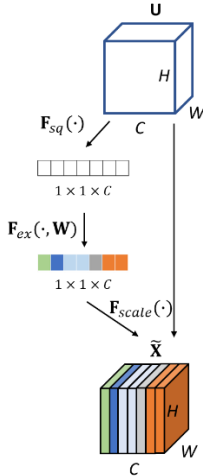


**FIGURE 13.** Squeeze-and-excitation block.

is  $s_i$ , it is generated by the weighted sum of all the hiddent states,

$$s_i = \sum_{t=1}^L w_{it} \mathbf{h}_t \quad (2)$$

where  $L$  is the maximum input sequence length. The weight  $w_{it}$  is computed by a softmax function as,

$$w_{it} = \frac{\exp(e_{it})}{\sum_{k=1}^L \exp(e_{ik})} \quad (3)$$

$$e_{it} = a(\mathbf{s}_{i-1}, \mathbf{h}_t)$$

where  $e_{it}$  is the energy of alignment described by the function  $a(\cdot)$ , which intends to capture the alignment between the input reading at  $t$  and output at  $i$ . In [16], the alignment model is parameterized by a feedforward neural network, and is trained jointly with other model components.

### B. SQUEEZE-AND-EXCITATION BLOCK

In order to take the distinct weights of different channels into account, a squeeze-and-excitation block (SENet) is stacked to the convolutional module of the classifier. SENet [17] was originally proposed to improve the expressing capability of network through explicitly modeling the interdependencies between feature channels, which is mainly governed by two key steps, namely squeeze and excitation, as illustrated in Fig. 13.

Suppose  $\mathbf{U}$  is the feature tensor transformed from input  $\mathbf{X}$  through  $\mathbf{F}_{tr}$ :  $\mathbf{X} \rightarrow \mathbf{U}$ ,  $\mathbf{X} \in \mathbb{R}^{W' \times H' \times C'}$ ,  $\mathbf{U} \in \mathbb{R}^{W \times H \times C}$ . Thus,  $\mathbf{U}$  is a tensor consisted of  $C$  feature maps, i.e.,  $\mathbf{U} = [\mathbf{u}_1, \mathbf{u}_2, \dots, \mathbf{u}_C]$ . Each channel is obtained by a standard convolutional operation as,

$$\mathbf{u}_c = \mathbf{v}_c * \mathbf{X} = \sum_{h=1}^{C'} \mathbf{v}_c^h * \mathbf{x}^h \quad (4)$$

where  $\mathbf{v}_c$  denotes the  $c$ -th kernel and  $\mathbf{x}^h$  stands for the  $h$ -th input.

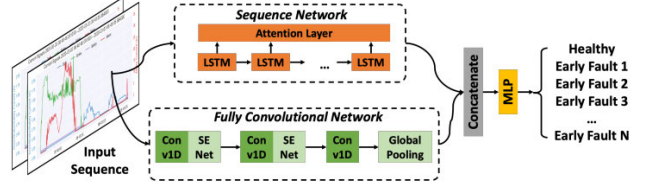


**FIGURE 14.** Architecture of MLSTM-FCN.

The squeeze operation  $\mathbf{F}_{sq}(\cdot)$  attempts to obtain the global distribution of channel-wise responses using a global average pooling. Given the sequence dataset in this problem, the feature map  $\mathbf{U}$  is shrunk through temporal dimensions,  $T$ , to calculate the channel-wise statistics,  $\mathbf{z} \in \mathbb{R}^C$ . Each element of  $\mathbf{z}$  is the channel-wise global average over the sequence length  $T$ , which is expressed by,

$$\mathbf{z}_c = \mathbf{F}_{sq}(\mathbf{u}_c) = \frac{1}{T} \sum_{t=1}^T \mathbf{u}_c(t) \quad (5)$$

Subsequently, an excite operation  $\mathbf{F}_{ex}(\cdot, \mathbf{W})$  is introduced to capture the channel-wise dependencies. To this end, the gating mechanism, which is similar to that of LSTM, is applied,

$$\mathbf{q} = \mathbf{F}_{ex}(\mathbf{z}, \mathbf{W}) = \sigma(g(\mathbf{z}, \mathbf{W})) = \sigma(\mathbf{W}_2 \delta(\mathbf{W}_1 \mathbf{z})) \quad (6)$$

where  $\mathbf{F}_{ex}(\cdot, \mathbf{W})$  can be viewed as a two-layered neural network. The first fully-connected layer with parameters  $\mathbf{W}_1$  and ReLU activation function  $\delta$  aims to reduce the dimensionality to  $C/r \times C$ , where  $r$  is the reduction ratio. As a result, the output dimensionality of first layer turns into  $1 \times 1 \times C/r$ , which essentially reduces the computational complexity. The output is then passed to the second fully-connected layer with parameters  $\mathbf{W}_2$  and Sigmoid activation function  $\sigma$ , where the dimensionality of  $\mathbf{W}_2$  is also  $C/r \times C$ . As such, the final output  $\mathbf{q}$  is derived with dimensionality of  $1 \times 1 \times C$ .  $\mathbf{W}_1$  and  $\mathbf{W}_2$  are jointly learned with other parameters in the network. As a matter of fact, the output  $\mathbf{q}$  is normalized weight vector corresponding to  $C$ -length feature map in  $\mathbf{U}$ .

Finally, we multiplied the obtained weights with each of the feature channels via a scale operation  $\mathbf{F}_{scale}(\cdot)$  as,

$$\tilde{\mathbf{x}}_c = \mathbf{F}_{scale}(\mathbf{u}_c, q_c) = q_c \cdot \mathbf{u}_c \quad (7)$$

### C. NETWORK ARCHITECTURE

The entire MLSTM-FCN model contains two branches, namely the sequence network and fully convolutional network, as illustrated in Fig. 14. The inputs are a collection of independent multivariate sequences that represent manifold operational scenarios. All inputs are fed into the model with shape  $(N, T, M)$ , where  $N$  is the number of samples,  $T$  is the maximum sequence length amongst all samples and  $M$  is the number of variables (i.e., channels in fully convolutional module). The sequence network is built upon LSTM units with attention mechanisms, which aims to exploit the temporal dependencies involved in the multivariate time series. The

**TABLE 3.** Number of Samples With Respect to Different Classes

Dataset	1_Healthy condition	2_Brake is not fully opened	3_Grid voltage dip	4_Door closing issue	Total
Train	19183	33	8	59	19283
Test	19184	27	12	61	19284
Total	38367	60	20	120	38567

convolutional block acts as a feature extractor, which is composed of three stacked temporal convolutional blocks [18] and a global pooling layer. Each block consists of a temporal convolutional layer (e.g., 1D convolutional layer) and SENet. Note that incorporation of SENet is essential to model performance enhancement [13], since it considers learned self-attention to the inter-correlations between multiple variables at each time step, given that not all feature maps has the same impact to the subsequent layers. The output of the sequence module and convolutional module are concatenated and passed onto a multilayer perceptron (MLP) with softmax activation function.

## V. EXPERIMENTS

As aforementioned in Section III, the whole dataset was divided into 38367 multivariate sequences covering three months, which are all deemed as normal conditions. The anomaly samples are collected either from simulations or real-life cases. Given the lift anomalies are rare in practice, we generated a handful of irregular current signals corresponding to each abnormality. Specifically, three abnormal events are considered, i.e., brake is not fully opened, grid voltage dip and door closing issue, with the anomaly number of 60, 20 and 120, respectively. The number of samples with respect to each class is listed in Table 3. Thus, the total number of samples is 38567 (i.e.,  $N = 38567$ ), each of them consists of 4 variables (i.e.,  $M = 4$ ). The maximum sequence length is 402 (i.e.,  $T = 402$ ). We used the former 50% for training and the remaining 50% is used for testing. Four classes regarding different operational conditions are considered in this study, namely healthy conditions, brake is not fully opened, grid voltage dip and door motor malfunctions.

Since the abnormal cases only account for 0.5% of whole dataset, a weighted learning strategy [19] was adopted in this model to mitigate such data imbalanced influence. Specifically, the loss function is weighted by the contribution of each class  $D_i$  ( $1 \leq i \leq D$ ) by the factor

$$G_{wi} = \frac{N}{D \cdot N_{D_i}} \quad (8)$$

where  $G_{wi}$  is the loss scaling weight for the  $i$ -th class,  $N$  is the number of samples,  $D$  is the number of classes and  $N_{D_i}$  is the number of samples belonging to class  $D$ . In addition, to have a consistent input length, post-sequence paddings with zeros are performed to the sequences with variable lengths.

The experiment was carried out on a single Nvidia GeForce GTX 2080Ti using Keras 2.2.4 [20] with Tensorflow backend in Python 3.6.4. The computer for implementation is

**TABLE 4.** Summary of Hyperparameters

Module	Hyperparameter	Value
Sequence Network	Number of LSTM cells	64
	Dropout	0.8
Fully Convolutional Network	Number of blocks	3
	Number of filters	128-256-128
	Kernel sizes	8-5-3
	Kernel initializer	he_uniform
	Activation function	ReLU
	Reduction ratio	16
MLP	MLP activation function	softmax
	Loss function	crossentropy
	Batch size	128
Others	Epochs	150
	Optimizer	Adam
	Learning rate	1.00E-03

equipped with a 3.6 GHz 8-core AMD Ryzen CPU and 64GB memory.

## A. MODEL SETTINGS

The number of LSTM cells in the sequence network is set as 64, in the meanwhile, we dropped some units out in the training phase for regularization, the dropout rate is set as 0.8. On the other hand, the fully convolutional network is consisted of three temporal convolutional blocks and a global average pooling layer, where the first two convolutional blocks are stacked by SENet. The convolutional blocks are configured with 128-256-128 filters, with kernel sizes of 8-5-3, respectively. The convolutional kernels are initialized by the Uniform He initialization scheme kernel [21] and the activation function is set as ReLU. For both SENets, the reduction ratio value is set to 16. The MLSTM-FCN is trained using a batch size of 128 over 150 epochs. Adam is selected as the optimizer with 1.00e-3 learning rate. All other hyperparameters of both networks are kept default as that in Tensorflow framework [22].

## B. METRICS

The performance of the MLSTM-FCN based classifier in dealing with elevator operational data was verified via the following metrics.

- **Precision:** this metric quantifies the number of positive class predictions that actually belong to the positive class, which is defined as,

$$\text{Precision} = \frac{\text{TruePositive}(TP)}{\text{TruePositive}(TP) + \text{FalsePositive}(FP)} \quad (9)$$

- **Recall:** this is defined by the number of positive class predictions made out of all positive samples in the dataset, which is expressed as,

$$\text{Recall} = \frac{\text{TruePositive}(TP)}{\text{TruePositive}(TP) + \text{FalseNegative}(FN)} \quad (10)$$

- **F1-Score:** this aims to provide a single score that balances both the concerns of precision and recall in one function.

**TABLE 5.** Confusion Matrix of Anomaly Sequence Detection Results

Classes	1_Healthy condition	2_Brake is not fully opened	3_Grid voltage dip	4_Door closing issue
1_Healthy condition	19163	0	0	9
2_Brake is not fully opened	0	27	0	0
3_Grid voltage dip	0	0	12	0
4_Door closing issue	21	0	0	52

**TABLE 6.** Performance Summary

Classes	Precision	Recall	F1-score	support
1_Healthy condition	0.9995	0.9989	0.9992	19184
2_Brake is not fully opened	1.000	1.000	1.000	27
3_Grid voltage dip	1.000	1.000	1.000	12
4_Door closing issue	0.7123	0.8525	0.7761	61

$$\text{F1Score} = 2 * \frac{\text{Precision} * \text{Recall}}{\text{Precision} + \text{Recall}} \quad (11)$$

All these metrics are positive-oriented with maximum value of 1, i.e., the model is more skillful if the values of indices are closer to 1. Note that ‘accuracy’ was not adopted as one of the evaluation indices in this experiment since the underlying dataset is highly imbalanced. Accuracy is essentially the total number of correct predictions divided by all predictions, which is meaningless when overwhelming number of samples are correctly predicted.

## C. RESULTS

The results of abnormality detection are shown in Table 5, where the row entries stand for true classes and the column entries represent the predicted outcomes belonging to each class. It is noticed that the MLSTM-FCN is highly skillful in distinguishing the underlying lift conditions. For healthy measurements, it only falsely estimates 21 cases out of 19184 total healthy conditions, leading to a high recall value of 0.9989 (see Table 6). It is also worthy noting that all the falsely detected labels belong to the door closing issues. By looking into these sequences, we did find that most of them behave quite similar to that when door has real closing issues, that is, it is difficult to distinguish the exact number of door current waveforms during door operation since sometimes the rapid door opening and closing manipulations would also yield the similar door current waveforms as that shown in Fig. 11 (b). On the other hand, among all predictions of healthy conditions, the only 9 false predictions also come from the class of door issues, resulting in a high precision of 0.9995, which further demonstrates the patterns

of door motion are sometimes similar in both normal and malfunctional situations. As for those measurements when brake is not fully opened or grid voltage experiences a dip, the MLSTM-FCN model can perfectly detect the respective patterns, while no false prediction is derived. Yet, the model performance slightly declines for the measurements with door closing problems, giving the precision and recall values of 0.7123 and 0.8521 respectively. In the meanwhile, the overall model performance with respect to each concerning condition is evaluated by F1-score, results further demonstrate that the underlying deep learning model is effective to identify the anomaly patterns or potential early faults of lifts based on the current signals of main components.

## VI. CONCLUSION

This work proposed a novel non-intrusive elevator well-being monitoring and fault diagnosis framework, which employs deep learning algorithm to learn the current signals of critical circuits of elevators. The current signals were acquired via clamp-on type current transformers, associated with a Raspberry PI. There will be no interventions to the circuitry or programmes of the elevators for the implementation of the proposed framework. The MLSTM-FCN model was employed to learn distinct patterns exhibited in manifold current profiles. Specifically, we considered three irregular situations and manually created a small amount of the faulty signals, the experiment demonstrated that the employed deep learning model is highly skillful in detecting these anomalies. The proposed framework enables maintenance contractors to carry out predictive maintenance at an early stage on lift installations for the rectification of potential faults and failures, especially for new and old lifts that requires monitoring of operating condition through an non-intrusive, low-cost and simple way.

Collection of faulty signals is the most challenging task in such supervised learning framework. Since the real faults are rare to occur in practice, simulation of the faults that are most likely to happen is of vital importance. Therefore, the diagnosis module will be enhanced for more fault advisories in the future study. In addition, the learning samples will be enriched by acquiring more related signals. One possible way is to explore the mechanic properties of elevator by adding more sensors, e.g., gyroscope, tachometer.

## ACKNOWLEDGMENT

The authors would like to express their special thanks of gratitude to the VTC Pro-Act Training and Development Centre (Electrical) team led by Charles Wong, Andy Lai, and Sunny Wong for their works in data labeling and fault simulation including the cases listed in “C. Generation of Abnormal Sequences” of Section III.

## REFERENCES

- [1] Y. Jia, Y. Gao, Z. Xu, K. P. Wong, L. L. Lai, Y. Xue, Z. Y. Dong, and D. J. Hill, “Powering China’s sustainable development with renewable energies: Current status and future trend,” *Electr. Power Compon. Syst.*, vol. 43, nos. 8–10, pp. 1193–1204, Jun. 2015.

- [2] S. Yin, S. X. Ding, X. Xie, and H. Luo, "A review on basic data-driven approaches for industrial process monitoring," *IEEE Trans. Ind. Electron.*, vol. 61, no. 11, pp. 6418–6428, Nov. 2014.
- [3] X. Dai and Z. Gao, "From model, signal to knowledge: A data-driven perspective of fault detection and diagnosis," *IEEE Trans. Ind. Informat.*, vol. 9, no. 4, pp. 2226–2238, Nov. 2013.
- [4] E. Esteban, O. Salgado, A. Iturrospe, and I. Isasa, "Model-based estimation of elevator rail friction forces," in *Proc. Int. Conf. Condition Monitor. Machinery Non-Stationary Operation*, vol. 4. Springer, 2014, pp. 363–374.
- [5] E. Esteban, O. Salgado, A. Iturrospe, and I. Isasa, "Model-based approach for elevator performance estimation," *Mech. Syst. Signal Process.*, vols. 68–69, pp. 125–137, Feb. 2016.
- [6] I. O. Olalere and M. Dewa, "Early fault detection of elevators using remote condition monitoring through IoT technology," *South Afr. J. Ind. Eng.*, vol. 29, no. 4, pp. 17–32, Dec. 2018.
- [7] J. Yan, M. Koç, and J. Lee, "A prognostic algorithm for machine performance assessment and its application," *Prod. Planning Control*, vol. 15, no. 8, pp. 796–801, Dec. 2004.
- [8] S. Yuan, M. Ge, H. Qiu, J. Lee, and Y. Xu, "Intelligent diagnosis in electromechanical operation systems," in *Proc. IEEE Int. Conf. Robot. Autom.*, vol. 3, Dec. 2004, pp. 2267–2272.
- [9] H.-M. Lei and G.-Y. Tian, "Broken wire detection in coated steel belts using the magnetic flux leakage method," *Insight-Non-Destructive Test. Condition Monitor.*, vol. 55, no. 3, pp. 126–131, Mar. 2013.
- [10] Z. Wan, S. Yi, K. Li, R. Tao, M. Gou, X. Li, and S. Guo, "Diagnosis of elevator faults with LS-SVM based on optimization by K-CV," *J. Electr. Comput. Eng.*, vol. 2015, pp. 1–8, Dec. 2015.
- [11] G. Niu, S.-S. Lee, B.-S. Yang, and S.-J. Lee, "Decision fusion system for fault diagnosis of elevator traction machine," *J. Mech. Sci. Technol.*, vol. 22, no. 1, pp. 85–95, Jan. 2008.
- [12] I. Skog, I. Karagiannis, A. B. Bergsten, J. Harden, L. Gustafsson, and P. Handel, "A smart sensor node for the Internet-of-elevators—Non-invasive condition and fault monitoring," *IEEE Sensors J.*, vol. 17, no. 16, pp. 5198–5208, Aug. 2017.
- [13] F. Karim, S. Majumdar, H. Darabi, and S. Harford, "Multivariate LSTM-FCNs for time series classification," *Neural Netw.*, vol. 116, pp. 237–245, Aug. 2019.
- [14] S. Hochreiter and J. Schmidhuber, "Long short-term memory," *Neural Comput.*, vol. 9, no. 8, pp. 1735–1780, 1997.
- [15] C. Fan, Y. Zhang, Y. Pan, X. Li, C. Zhang, R. Yuan, D. Wu, W. Wang, J. Pei, and H. Huang, "Multi-horizon time series forecasting with temporal attention learning," in *Proc. 25th ACM SIGKDD Int. Conf. Knowl. Discovery Data Mining*, Jul. 2019, pp. 2527–2535.
- [16] D. Bahdanau, K. Cho, and Y. Bengio, "Neural machine translation by jointly learning to align and translate," 2014, *arXiv:1409.0473*. [Online]. Available: <http://arxiv.org/abs/1409.0473>
- [17] J. Hu, L. Shen, and G. Sun, "Squeeze- and-excitation networks," in *Proc. IEEE/CVF Conf. Comput. Vis. Pattern Recognit.*, Jun. 2018, pp. 7132–7141.
- [18] Z. Wang, W. Yan, and T. Oates, "Time series classification from scratch with deep neural networks: A strong baseline," in *Proc. Int. Joint Conf. Neural Netw. (IJCNN)*, May 2017, pp. 1578–1585.
- [19] G. King and L. Zeng, "Logistic regression in rare events data," *Political Anal.*, vol. 9, no. 2, pp. 137–163, 2001.
- [20] F. Chollet et al. *Keras*. Accessed: Nov. 17, 2020. [Online]. Available: <https://github.com/keras-team/keras>
- [21] K. He, X. Zhang, S. Ren, and J. Sun, "Delving deep into rectifiers: Surpassing human-level performance on ImageNet classification," in *Proc. IEEE Int. Conf. Comput. Vis. (ICCV)*, Dec. 2015, pp. 1026–1034.
- [22] M. Abadi, P. Barham, J. Chen, Z. Chen, A. Davis, J. Dean, M. Devin, S. Ghemawat, G. Irving, M. Isard, and M. Kudlur, "Tensorflow: A system for large-scale machine learning," in *Proc. 12th USENIX Symp. Operating Syst. Design Implement.*, 2016, pp. 265–283.

• • •